Effect of Adhesive Layer Thickness and Slant Angle on Piezoelectric Bonded Joints

Somnath Somadder, Md. Shahidul Islam*
Department of Mechanical Engineering,
Khulna University of Engineering & Technology,
Khulna-9203, Bangladesh
**somnath@me.kuet.ac.bd*

ABSTRACT

Piezoelectric materials have found their parts in numerous manufacturing applications such as transducers and sensors. Piezoelectric material shows anisotropy; in addition, its elastic field and electric field are integrated. The analysis of piezoelectric materials has obtained great interest among researchers with the development of smart structures. It is significant to explain the distribution of stress and electric displacement fields along the bonded edge. It has never been obvious how stress singularity and electric displacement fields are distributed at the vertex of piezoelectric dissimilar material joints. Stress and electric displacement distribution near the vertex along the interface of piezoelectric boned joints are investigated in this present research. Numerical analysis of piezoelectric dissimilar material joints is carried out by using Abaqus FEA software. From the numerical analysis, it is observed that stress, displacement, electric potential, electric displacement field evolvement along the interface edge rises with the increment of adhesive layer thickness and slant angle. So, a thin adhesive layer thickness and small slant angle are more reliable for operation.

Keywords: *Piezoelectric Material, Smart Structure, Slant Angle, Dissimilar Material Joints, Singular Stress Components*

Introduction

An adhesive Bonded joint denotes a durable joint by joining the adherents through an adhesive that creates a bond between the surfaces. Bonded joints do not generate local stress concentrations which can cause material failure

ISSN 1823-5514, eISSN 2550-164X
Received for review: 2021-07-14
Accepted for publication: 2021-12-06
Published: 2022-04-15

into layers through the thickness of the adherend compared to mechanical joints. Furthermore, they are much lighter than mechanical joints. Enormous research based on the bonded joint can be found. Hideo Koguchi [1] analyzed stress singularity which is considered a novel approach in the bonded joint analysis.

A comparison of modeling and simulation of piezoelectric elements was carried out by Michal Staworko and Tadeusz Uhl [2]. The intensity of residual thermal stress is analyzed by Hideo Koguchi and N. Konno [3]. The piezoelectric effect was investigated numerically by Sefer Avdiaj et al. [4]. The three-dimensional piezoelectric isogeometric finite element was developed by Willberg, Gabbert [5]. The Eigen analysis method was used by Md. Shahidul Islam et al. [6] to determine the order of stress singularity at a vertex in 3D transversely isotropic piezoelectric single step bonded joints. Md. Shahidul Islam and Hideo Koguchi [7] utilized BEM to obtain the intensities of stress singularities. A numerical investigation of PZT materials by using FEM was carried out by Chetan Byrappa et al. [8]. A singular electric flux density occurs in piezoelectric bonded joints at the vertex of the interface when mechanical compression or electrical load was applied. The effect of the mechanical or electrical load was examined by Hideo Koguchi et al. [9]. An analytical and numerical model was established to obtain the output voltage of the PZT energy harvester by Zubair Butt et al. [10]. A numerical investigation of isotropic elastic bonded joints using Eigen analysis was carried out by Md. Shahidul Islam et al. [11].

The Conservative integral approach was used by Chonlada Luangarpa and Hideo Koguchi [12] to calculate the stress intensity of the piezoelectric bonded joint. A cantilever beam with PZT patches was analyzed by Shubham Padalkar et al. [13] using Abaqus. Stress analysis of functionally graded piezoelectric material via shear deformation theory is done by Zenkour and Alghanmi [14]. Two perfectly bonded joints, which were different inside the surface shape, were investigated to determine the order of stress singularity using the finite element method by Chonlada Luangarpa and Hideo Koguchi [15]. An analytical model was developed for piezoelectric beams under small strain but large displacements by Neto et al. [16]. The effect of slant angle on the piezoelectric bonded joint is investigated by Somnath Somadder and Md. Shahidul Islam [17]. Electrostatic analysis of three-dimensional piezoelectric elements using the finite difference method was carried out by Hao Xia and Yan Gu [18]. Dynamic stress analysis of a piezoelectric bi-material strip is carried out by Hui Qi et al. [19].

The main focus of the present work is to inspect the singular stress, displacement, electric potential, electric displacement field effect with interlayer thickness, and slant angle in piezoelectric dissimilar material joints.

Mathematical Modelling

To define piezoelectric materials in Abaqus FEA various material parameter like the elastic constant, piezoelectric constant, and dielectric constant is required. It is extremely hard to obtain an analytical solution for piezoelectric materials because of their complicated governing equations. In Abaqus, the following constitutive equations are used [20]

$$\sigma_{ij} = D^{E}_{ijkl}\varepsilon_{kl} - e^{\phi}_{mij}E_{m} \tag{1}$$

$$q_{i} = e^{\phi}_{ijk}\varepsilon_{jkl} + D^{\phi(\varepsilon)}_{ij}E_{j} \tag{2}$$

D_{ijkl} indicates the material stiffness; e^{ϕ}_{ijk} denotes piezoelectric constant and D^{ϕ}_{ij} is the dielectric constant. The mechanical equilibrium equation is given by [21].

$$\int_{V} \sigma : \delta\varepsilon dV = \int_{S} t.\delta u dS + \int_{V} f.\delta u dV \tag{3}$$

where $\delta\varepsilon \overset{def}{=} sym\dfrac{\partial\delta u}{\partial x}$, and δu is taken as an arbitrary vector field and every component is continuous. The electrical flux conservation equation is written as,

$$\int_{V} q.\delta E dV = \int_{S} q_{S}\delta\phi dS + \int_{V} q_{v}\delta\phi dV \tag{4}$$

Where $\delta E \overset{def}{=} sym\dfrac{\partial\delta\phi}{\partial x}$, and $\delta\phi$ is an arbitrary scalar field, which is considered to be continuous. The finite element discretization is conducted, which estimates the following solution [22]:

$$\begin{aligned} u_{c} &= N^{T}_{u}.u \\ V_{c} &= N^{T}_{V}.V \end{aligned} \tag{5}$$

where N_{u} denotes shape functions related to displacement, N_{V} indicates shape function related to electrical potential. Using Equation (5), Strain S and electrical field E can be obtained as,

$$S = B_u.u \tag{6}$$

$$E = B_V.V \tag{7}$$

where,

$$B_u = \begin{bmatrix} \frac{\partial}{\partial x} & 0 & 0 & \frac{\partial}{\partial y} & 0 & \frac{\partial}{\partial z} \\ 0 & \frac{\partial}{\partial y} & 0 & \frac{\partial}{\partial x} & \frac{\partial}{\partial z} & 0 \\ 0 & 0 & \frac{\partial}{\partial z} & 0 & \frac{\partial}{\partial y} & \frac{\partial}{\partial x} \end{bmatrix}^T, \tag{8}$$

$$B_V = \begin{bmatrix} \frac{\partial}{\partial x} & \frac{\partial}{\partial y} & \frac{\partial}{\partial z} \end{bmatrix}^T$$

The variational principle is employed to derive the finite element matrix equation and the finite element discretization,

$$\begin{bmatrix} M & 0 \\ 0 & 0 \end{bmatrix} \begin{bmatrix} \ddot{u} \\ \ddot{V} \end{bmatrix} + \begin{bmatrix} C & 0 \\ 0 & 0 \end{bmatrix} \begin{bmatrix} \dot{u} \\ \dot{V} \end{bmatrix} + \begin{bmatrix} K & K_z \\ K_z^T & K_d \end{bmatrix} \begin{bmatrix} u \\ V \end{bmatrix} = \begin{bmatrix} F \\ L \end{bmatrix} \tag{9}$$

where,

Structural Mass is indicated by $M = \int \rho N_u N_u^T dV$

Structural Stiffness is denoted by $K = \int B_u^T C B_u dV$

C is the structural damping matrix. Piezoelectric coupling matrix is expressed as follows $K_z = \int B_u^T e B_u dV$

Dielectric conductivity is denoted by $K_d = \int B_V^T \varepsilon B_V dV$

FEM modelling

Abaqus 6.14 finite element software is used to create FEM. To observe the effect of slant angle and adhesive layer thickness model in Figures 1 and 2 is used respectively. The dimensions of the model are shown in Figures 1 and 2. By taking advantage of symmetry, one-fourth of the model will be analyzed. This is done to decrease computational time with proper mesh size. The lower

surface of the model is kept fixed; 1 MPa force and 1 C are applied at the upper surface. Adhesive layer thickness t and slant angle α are varied to observe its effect on singular stress, displacement, electric potential, electric displacement field.

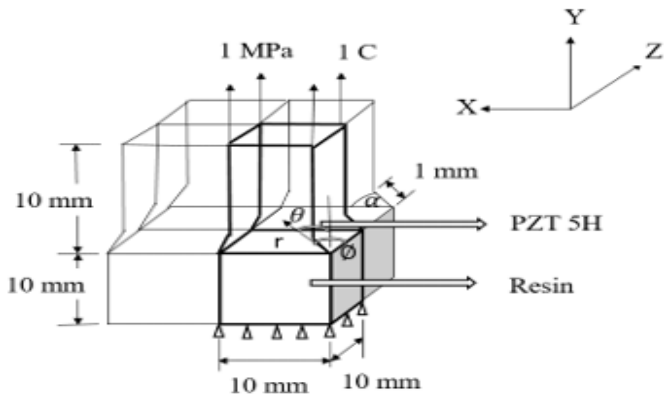

Figure 1: Model of investigation (considering the effect of slant angle)

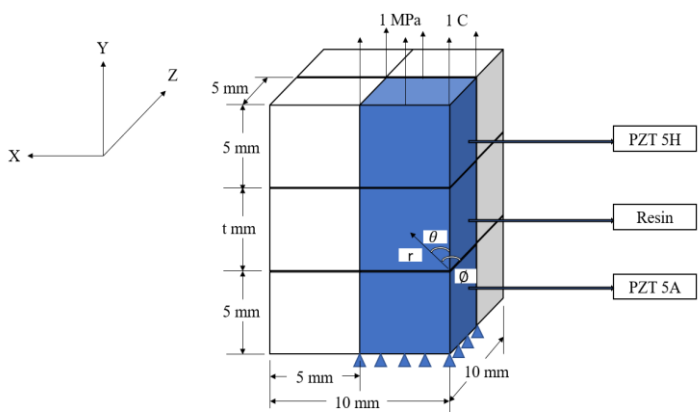

Figure 2: Model of investigation (considering the effect of interlayer thickness)

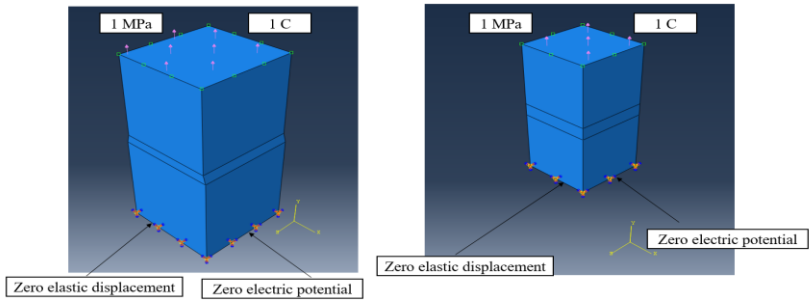

(a) (b)

Figure 3: Model showing the boundary conditions of the analysis (a) considering the effect of slant angle, (b) considering the effect of interlayer thickness

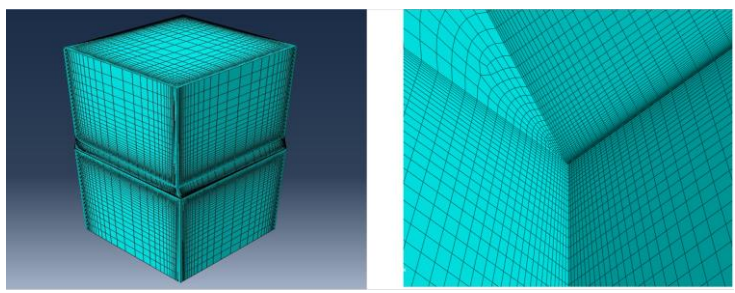

(a) (b)

Figure 4: Mesh of the model (a) considering the effect of slant angle (b) zoomed view near the vertex

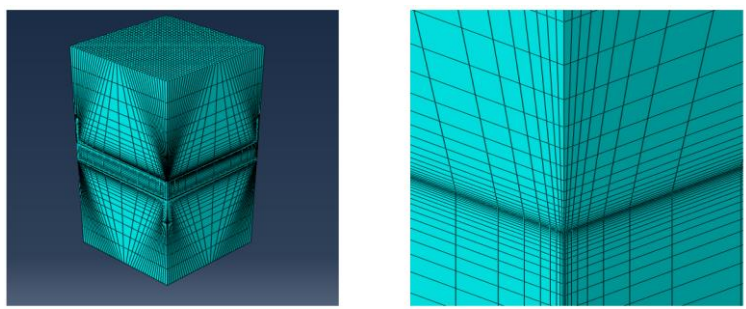

(a) (b)

Figure 5: Mesh of the model (a) considering the effect of the interlayer thickness (b) zoomed view near the vertex

High stress generates near the vertex of the piezoelectric bonded joints. Therefore vertex is the critical region and biasing has been done so there are more elements near the vertex than in the other regions. Double bias is used on the horizontal edges and single bias is used on vertical edges. In case of bias, the minimum size is taken as 0.0001 mm and the maximum size is taken as 1 mm. As this is a 3D piezoelectric analysis, 8 nodes linear piezoelectric brick element C3D8E is used in this analysis.

Material characteristics

The material attributes of piezoelectric materials PZT 5H, PZT 5A, and resin are given in Table 1.

Table 1: Material attributes of PZT 5H [23], PZT 5A [24], and resin [25]

Material	**Elastic Constant, 10^{10} N/m^2**					**Piezoelectric Constant, 10^{-12} m/volt**			**Dielectric constant, 10^{-8} F/m**	
	c_{11}	c_{12}	c_{13}	c_{33}	c_{44}	d_{15}	d_{31}	d_{33}	ξ_{11}	ξ_{33}
PZT 5H	12.60	7.95	8.41	11.70	2.30	741	-274	593	2.771	3.0104
PZT 5A	12.10	7.54	7.52	11.10	2.11	584	-171	374	1.5317	1.5052
Resin	10.40	5.11	5.11	10.40	2.63	0	0	0	0.3790	0.3790

Numerical Result and Discussion

In this research, Abaqus 6.14 commercial software was utilized to investigate the impact of adhesive layer thickness and slant side surface on singular stress field, electric displacement, electric potential, displacement in piezoelectric bonded joint. The components of displacement, stress, electric potential, electric displacement is plotted against r, θ, ϕ.

For the verification of this research work, the result obtained from running the commercial code using Abaqus FEA software is compared to the result of Hideo Koguchi and Joviano Antonio Da Costa [26]. The results achieved in the present analysis are in good concurrence with the reference paper results where the highest error percentage is less than 1%.

From mesh sensitivity analysis, the results obtained using 5,22,376 elements are similar to the results obtained using 6,18,142 elements. To save the time of calculation the optimum number of elements for further analysis is 5,22,376 elements.

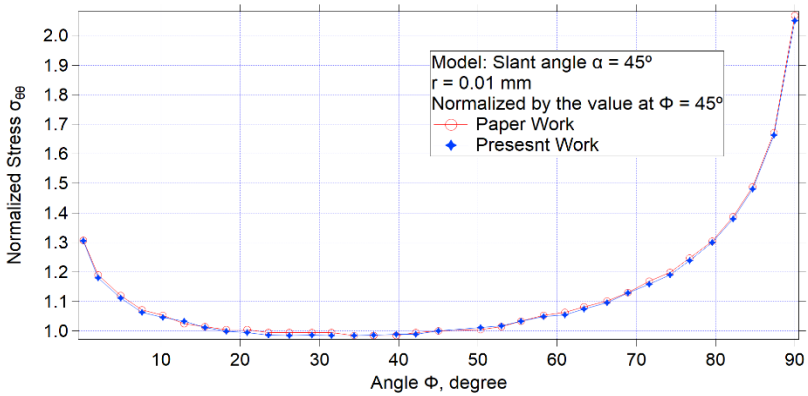

Figure 6: Comparision of present analysis with reference paper analysis for the variation of normalized stress $\sigma_{\theta\theta}$ against angle ϕ

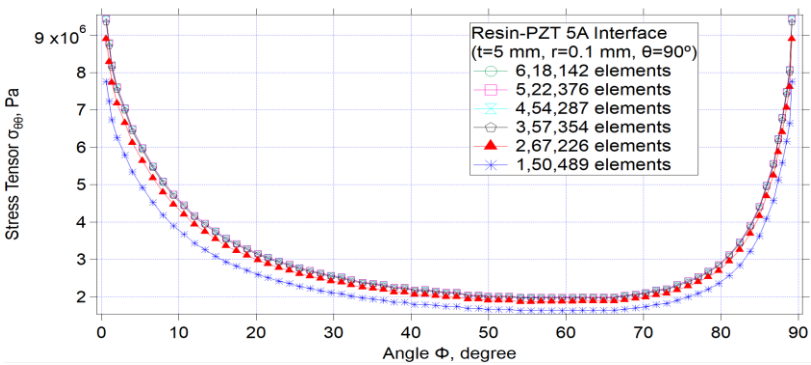

Figure 7: Mesh convergence check for the current model

Figure 8 shows the 3D surface plot of displacement components and electric potential against radial distance and the angle ϕ at the Resin-PZT 5A interface for the t=1 mm model. From the distribution of the elastic displacement component u_θ, it is clear that elastic displacement decreases with the increase of radial distance from the vertex. It is observed all the components have higher values adjacent to the vertex and in the way of interface, boundary compared to other areas.

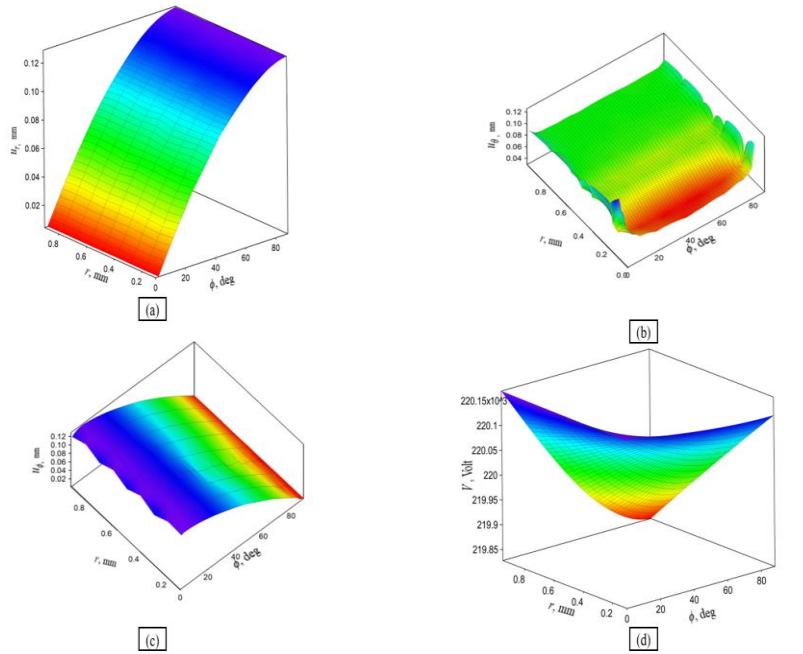

Figure 8: Variation of elastic displacement (a) u_r (b) u_θ (c) u_ϕ (d) electric potential V against r and ϕ at Resin-PZT 5A interface for t=1 mm mode

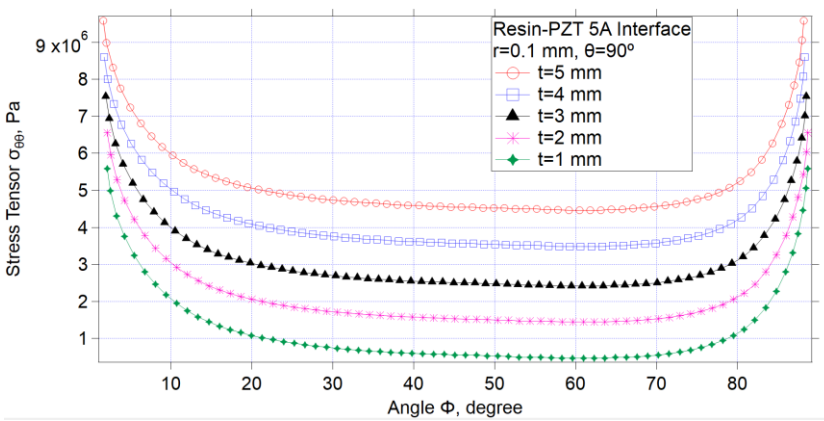

Figure 9: Variation of stress tensor $\sigma_{\theta\theta}$ against angle ϕ for various adhesive layer thicknesses.

Figure 9 represents the variation of stress components $\sigma_{\theta\theta}$ respectively against angle ϕ for various adhesive layer thicknesses. From the figure, it is observed that stress tensor $\sigma_{\theta\theta}$ has relatively larger values at ϕ=0° and ϕ =90° which is at the interface edge. The graph is nearly symmetric at ϕ=45°. With the increment of adhesive layer thickness, stress tensor $\sigma_{\theta\theta}$ increases. Among five different models, stress evolvement is the highest for the t = 5 mm model and lowest for the t = 1 mm model. The order of stress singularity and stress intensity increases with the increase of adhesive layer thickness.

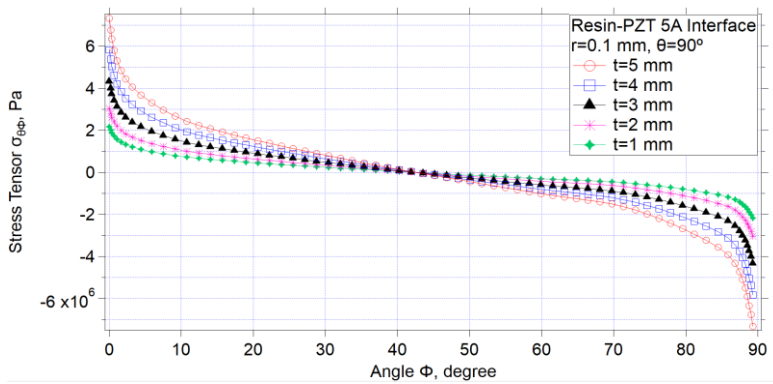

Figure 10: Variation of stress tensor $\sigma_{\theta\phi}$ against angle ϕ for various adhesive layer thicknesses

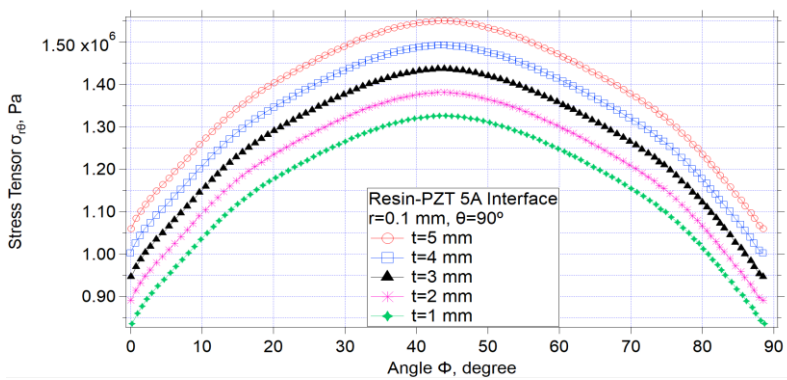

Figure 11: Variation of stress tensor $\sigma_{r\theta}$ against angle ϕ for various adhesive layer thicknesses

Figures 10 and 11 represents the distribution of stress component $\sigma_{\theta\phi}$ and $\sigma_{r\theta}$ against angle ϕ for various adhesive layer thickness. From figure 10, it is observed that the stress tensor $\sigma_{\theta\phi}$ has relatively larger values at ϕ =0° and ϕ=90° which is at the interface edge. The graph is nearly antisymmetric at ϕ=45°. With the increment of interlayer thickness, the magnitude of stress tensor $\sigma_{\theta\phi}$ and $\sigma_{r\theta}$ increases. Among five different models, stress evolvement is the highest for the t = 5 mm model and lowest for the t = 1 mm model. The order of stress singularity and stress intensity increases with the increase of adhesive layer thickness.

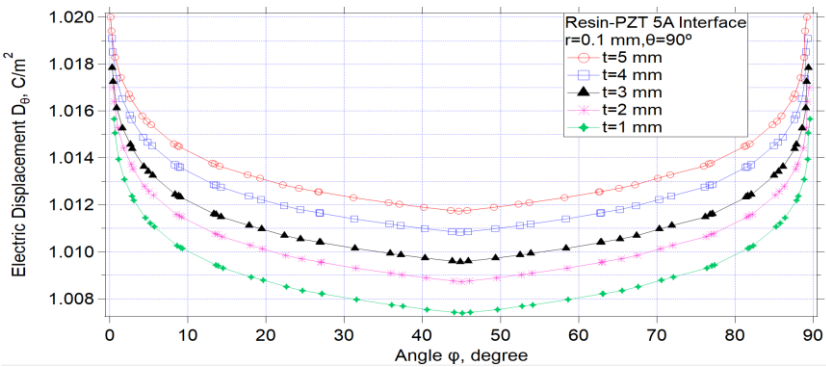

Figure 12: Variation of electric displacement D_θ against angle ϕ for various adhesive layer thicknesses

Figure 12 represents the variation of electric displacement D_θ against angle ϕ for various adhesive layer thicknesses. From figure 12, it is observed that electric displacement D_θ has relatively larger values at ϕ=0° and ϕ=90° which is at the interface edge. The graph is nearly symmetric at ϕ=45°. With the increment of interlayer thickness, the magnitude of electric displacement D_θ increases. The singularities associated with electric fields are also important. Among five different models, electric displacement evolvement is the highest for the t = 5 mm model and lowest for the t = 1 mm model.

Figure 13 shows the 3D surface plot of displacement components and electric potential against radial distance and the angle ϕ at the Resin-PZT 5H interface for the t=1 mm model. The distribution of elastic displacement

component u_θ has relatively larger values at ϕ=0° and ϕ=90° which is at the interface edge. It is observed all the components have higher values adjacent to the vertex and in the way of interface boundary compared to other areas.

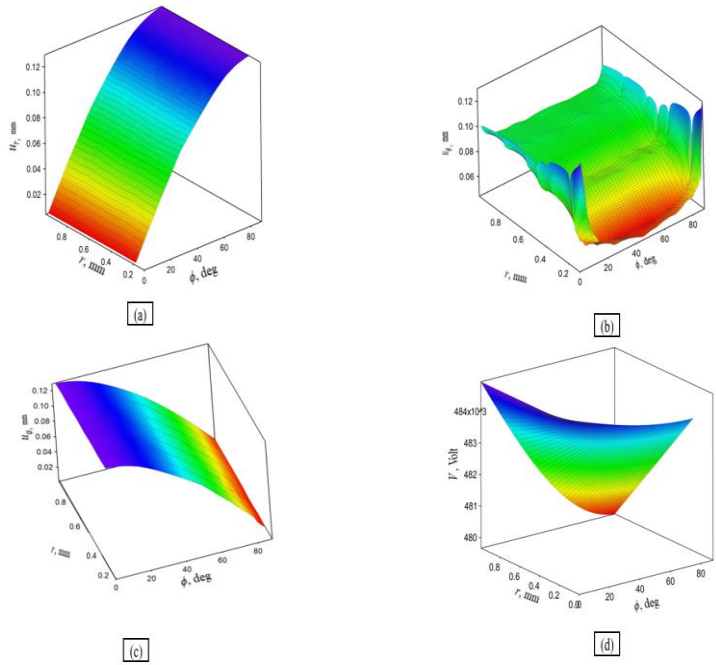

Figure 13: Variation of elastic displacement (a) u_r (b) u_θ (c) u_ϕ (d) electric potential V against r and ϕ at Resin-PZT 5H interface for t=1 mm model

Figure 14 and 15 represents the evolvement of stress tensor $\sigma_{\theta\theta}$ and electric displacement D_θ against angle θ for various interlayer thickness. It is clearly noted that stress and electric displacement distribution is continuous at the interface at $\theta = 90°$. Among five different models, stress tensor and electric displacement evolvement are the highest for the t = 5 mm model and lowest for the t = 1 mm model. The order of stress singularity and stress intensity increases with the increase of adhesive layer thickness.

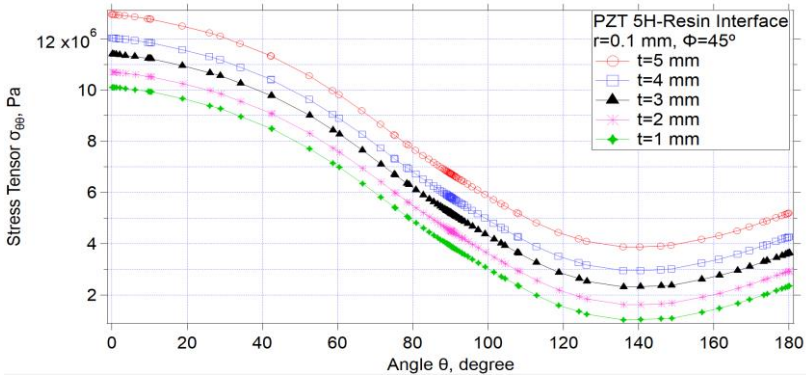

Figure 14: Variation of stress tensor $\sigma_{\theta\theta}$ against angle θ for various adhesive layer thicknesses

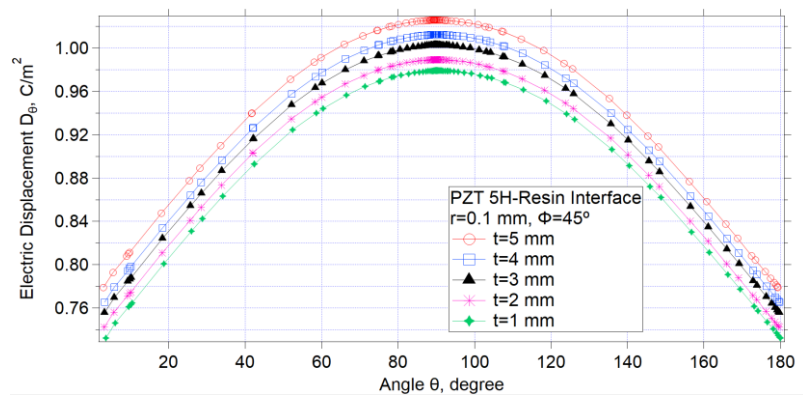

Figure 15: Variation of electric displacement D_θ against angle θ for various adhesive layer thicknesses

Figure 16 shows the 3D surface plot of displacement components and electric potential against radial distance and the angle ϕ at the Resin-PZT 5H interface for the slant 30° model. From the distribution of the elastic displacement component u_θ, it is clear that elastic displacement decreases with the increase of radial distance from the vertex and u_θ has relatively larger values at ϕ =0° and ϕ =90° which is at the interface edge. It is observed all the components have higher values adjacent to the vertex and in the way of interface, boundary compared to other areas.

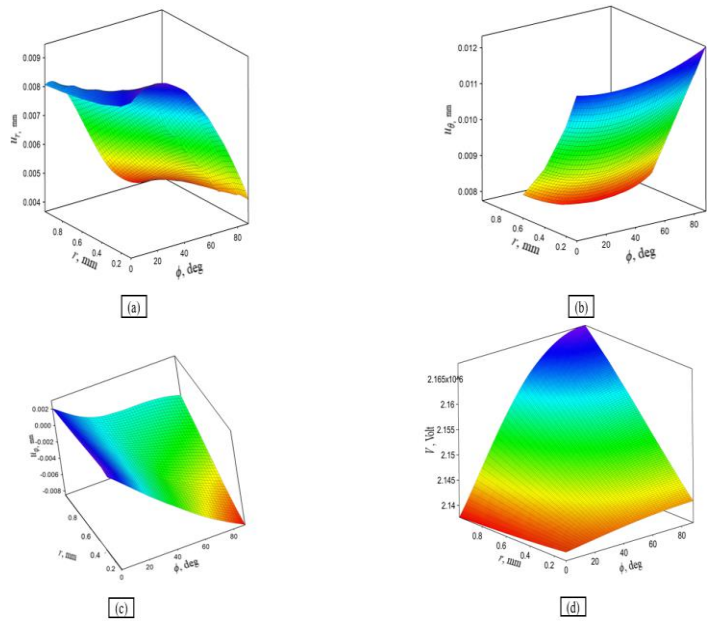

Figure 16: Variation of elastic displacement (a) u_r (b) u_θ (c) u_ϕ (d) electric potential V against r and ϕ at PZT 5H-Resin interface for slant 30° model

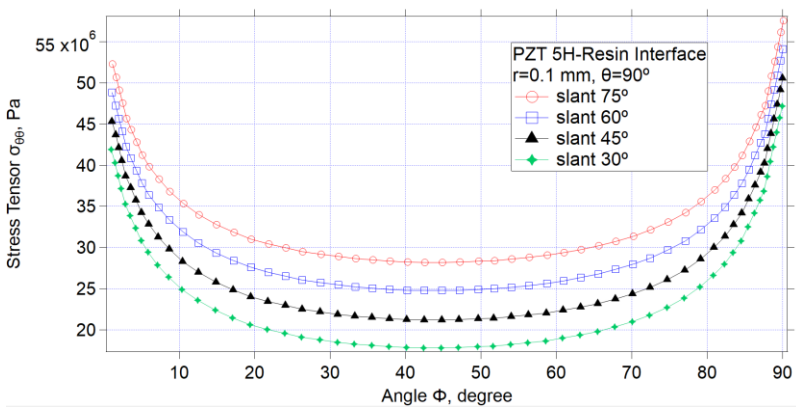

Figure 17: Variation of stress tensor $\sigma_{\theta\theta}$ against angle ϕ for various slant angles

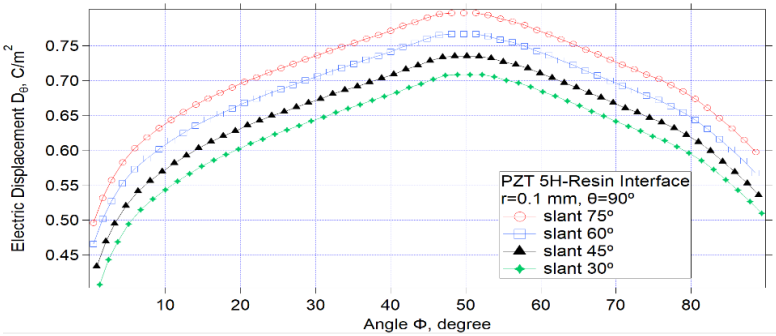

Figure 18: Variation of electric displacement D_θ against angle ϕ for various slant angles

Figure 17 and Figure 18 represents the variation of stress tensor $\sigma_{\theta\theta}$ and electric displacement field D_θ respectively against angle ϕ for various slant angle. Figure 17 denotes that large stress development near the vertex and interface edge is prevented by using a slanted side surface. Among four different models, stress and electric displacement evolvement are the highest for the slant 75° model and the lowest for the slant 30° model. The order of stress singularity and stress intensity increases with the increase of slant angle.

Conclusion

In this research, bi-material and tri-material piezoelectric bonded joints were analyzed using finite element analysis. Adhesive layer thickness and slant angle were varied to investigate its influence on the propagation of singular stress, displacement, electric potential, electric displacement field. The subsequent outcomes can be drawn as follows:

a) Maximum stress and electric displacement field takes place adjacent to the vertex and in the way of interface boundary compared to other areas.
b) Large stress and electric displacement field evolvements along the interface edge are disallowed by using a small slant angle. After analyzing models having different slant angles (α =75°, α =60° , α =45° , α =30°) it can be concluded that the slant 30° model is more suitable for operation.
c) Stress and electric displacement field-effect rise with the increment in adhesive layer thickness. After analyzing models having different adhesive layer thicknesses (t=1 mm, t=2 mm, t=3 mm, t=4 mm, t=5 mm) it can be concluded that the t=1 mm model is more suitable for operation.

References

[1] H. Koguchi, "Stress singularity analysis in three-dimensional bonded structure," Int. J. Solids Structures, vol. 34, pp. 461-480, 1997, doi: 10.1016/s0020-7683(96)00028-5.

[2] M. Staworko and T. Uhl, "Modeling and simulation of piezoelectric elements- comparison of available methods and techniques," Mechanics, vol. 27, pp. 161-170, 2008.

[3] H. Koguchi, N. Konno, "Intensity of residual thermal stresses at the vertex in three-dimensional joints with three layers," Society of Mechanical Engineers, Series A, vol. 75, pp.1148-1155, 2009, doi: 10.1299/kikaia.75.1148.

[4] S. Avdiaj, J. Setina, N. Syla, "Modeling of the piezoelectric effect using finite element method (FEM)," Materials and Technology, vol. 43, pp. 283-291, 2009.

[5] C. Willberg, U. Gabbert, "Development of a three-dimensional piezoelectric isogeometric finite element for smart structure applications," Acta Mechanica, vol. 223, pp.1837-1850, 2012, doi: 10.1007/s00707-012-0644-x.

[6] Md. S. Islam, Md. G. Kader, Md. K. Uddin, M. Ahmed, "Analysis of Order of Singularity at a Vertex in 3D Transversely Isotropic Piezoelectric Single-Step Bonded Joints," American Journal of Engineering Research, vol. 2, pp.v87-99, 2013.

[7] Md. S. Islam, H. Koguchi, "Analysis of intensity of singularity at a vertex in 3D transversely isotropic piezoelectric bi-material joints by boundary element method," 2nd International Conference on Informatics, Electronics and Vision, 2013.

[8] C. Byrappa, U. D. Prajwal, A. Kumar, "Study of Numerical Analysis on Piezoelectric Materials," International Journal of Engineering Research and Technology, vol. 7, pp. 145-152, 2014.

[9] H. Koguchi, T. Maekawa, C. Luangarpa "Investigation on singular fields at vertex of interface in piezoelectric material joints and its application," Proceedings of the ASME 2015 International Technical Conference and Exhibition on Packaging and Integration of Electronic and Photonic Microsystems, San Francisco, California, USA, 2015.

[10] Z. Butt, R. A. Pasha, F. Qayyum, Z. Anjum, N. Ahmad, H. Elahi, "Generation of electrical energy using lead zirconate titanate (PZT -5A) piezoelectric material: Analytical, numerical, experimental verifications," Journal of Mechanical Science and Technology, vol. 30, pp. 3553-3558, 2016, doi: 10.1007/s12206-016-0715-3.

[11] Md. S. Islam, M. Morshed, A.H.M. Mamun, "Evaluation of stress field at the vertex of the interface in three-dimensional dissimilar material joints," Int. Journal of Mechanical and Production Engineering,, IRAJ, vol. 6, pp. 24-30, 2018.

[12] C. Luangarpa, H. Koguchi, "Evaluation of intensities of singularity at three-dimensional piezoelectric bonded joints using a conservative integral," European Journal of Mechanics / A Solids, vol. 72, pp. 198-208, 2018, doi: 10.1016/j.euromechsol.2018.05.012.
[13] S. Padalkar, Y. Patil, G. Joshi, "Analysis of Cantilever Beam with PZT Patches in Abaqus," International Research Journal of Engineering & Technology, vol. 6, pp 4847-4848, 2019.
[14] A. M. Zenkour, R. A. Alghanmi, "Stress analysis of a functionally graded plate integrated with piezoelectric faces via a four-unknown shear deformation theory," Results in Physics, vol. 12, pp.268-277,2019, doi: 10.1016/j.rinp.2018.11.045.
[15] C. Luangarpa, H. Koguchi, "Singular Stresses at a Vertex and Along a Singular Line in Three Dimensional Piezoelectric Bonded Joints," Journal of Applied and Computational Mechanics, vol. 6, pp. 1364-1370, 2020, DOI: 10.22055/JACM.2020.33956.2379
[16] A. L. C. Neto, R.R.F. Santos, E. L. Neto, F. A. C. Monterio, "Piezoelectric beams under small strains but large displacements and rotations," Applied Mathematical Modeling, vol. 87, pp. 430-445, 2020, doi: 10.1016/j.apm.2020.05.029.
[17] S. Somadder, Md. S. Islam, "Effect of slant angle on piezoelectric boned joint" 6th International Conference on Mechanical, Industrial and Energy Engineering, 2020.
[18] H. Xia, Y. Guo, "Generalized finite difference method for electro elastic analysis of three-dimensional piezoelectric structures," Applied Mathematics Letter, vol. 117, 2021, doi: 10.1016/j.aml.2021.107084.
[19] H. Qui, X. M. Zhang, J. Yang, "The dynamic stress analysis of a piezoelectric bi-material strip with an inclusion," Waves in Random and Complex Media, vol. 31, 2021, doi: 10.1080/17455030.2019.1600767.
[20] T. Ikeda, "Fundamentals of Piezoelectricity," Oxford University Press, New York, 1990.
[21] Abaqus Theroy Manual, Section 2.10 "Piezoelectric analysis", Dassault Systems Simulia Corp., Providence, RI, USA, 2011.
[22] D. Popovici, F. Constantinescu, M. Maricaru, F. I. Hantila, M. Nitescu, and A. Gheorghe, "Modeling and simulation of piezoelectric devices," in Modeling and Simulation, G. Petrone and G. Cammarata, Eds., pp. 472–500, Intech, Rijeka, Croatia, 2008.
[23] https://www.efunda.com/materials/piezo/material_data/matdata_output.cfm?Material_ID=PZT-5H
[24] https://www.efunda.com/materials/piezo/material_data/matdata_output.cfm?Material_ID=PZT-5A
[25] Md. S. Islam, H. Koguchi, "Effect of Singularity at vertex of Transversely Isotropic Piezoelectric Dissimilar Material Joints," The Proceedings of Conference of Hokuriku-Shinetsu Branch, vol. 47, pp. 293-294, 2010, doi: 10.1299/jsmehs.2010.47.293.

[26] H. Koguchi, J. A. D. Costa, "Analysis of the stress singular field at a vertex in 3D bonded structures having a slanted surface," International Journal of Solids and Structures, vol. 47, pp. 3131-3140, 2010, doi: 10.1016/j.ijsolstr.2010.07.015.